Hybrid Broadband 60-GHz Double Negative Metamaterial High Gain Antenna

Taieb Elkarkraoui[1, *], Gilles Y. Delisle[1], Nadir Hakem[2], and Yacouba Coulibaly[2]

Abstract—This paper proposes a double negative metamaterial surface as a superstrate for a multilayer cylindrical dielectric resonator antenna (MCDRA). The aim is to achieve a broadband and high gain Electromagnetic Band Gap (EBG) antenna that can be used in harsh propagation areas to satisfy all the requirements for the 60 GHz wireless communications offering a bandwidth of 7 GHz in the unlicensed ISM band (57–65 GHz), permitting to reach data rates of 10 Gbit/s and more. To meet these objectives various techniques are combined. Numerical and experimental results showed satisfactory performances with achievable impedance bandwidth of more than 10.5% (from 58.1 to 64.2 GHz) and a 18 dBi gain, an enhancement of 13 dBi compared to a homogenous DRA without metamaterial superstrate. The proposed antenna exhibits directive and stable radiation pattern in the entire operating band.

1. INTRODUCTION

Good communication system in harsh industrial environment, in particular underground mines, can largely increase safety and production output. Unfortunately, it has been a neglected area in the mining industry mainly due to the difficulties of implementing such system and the high cost involved. The demands of high data rates have become important requirements for these underground communications systems. Today's wireless data rates at microwave frequencies and below are limited to about 1 Gbit/s. However, the demand for wireless 2 to 10 Gbit/s data rate systems will increase rapidly in the near future due to the introduction of advanced 4G systems and, ultimately, 5G technologies. Current wireless systems are not able to support this high data rates due to their limited bandwidth, thus the millimeter wave communication systems such as ISM 60 GHz band which offers 7 GHz of bandwidth, is one of the most direct and easiest ways to achieve such high data rate of 1–10 Gbit [1]. However, millimeter wave communications at frequencies around 60 GHz suffer from high insertion losses due to absorption by the oxygen molecules in the atmosphere [2]. Antennas with a high gain and broadband can be used to satisfy all the requirements for the 60 GHz wireless communications. Dielectric Resonators antennas (DRA) has been recently proposed as a solution to challenge the design of antennas for low cost systems to be used in the 60 GHz unlicensed frequency band. Numerous investigations have been carried out on dielectric resonator antennas (DRAs) in last two decades because of their favorable characteristics, such as small size, light weight, low profile, compact structure and simple feeding mechanism [3]. The two most serious limitations of the DRAs are its low gain and narrow bandwidth. Recently, various configurations of superstrate were used to enhance the gain of DRAs antennas such as dielectric slabs [4], electromagnetic band gap (EBG) structures [5, 6], highly-reflective surfaces [7], and most recently, metamaterial superstrate [8, 9]. The bandwidth of DRAs is also limited for single mode operation and this bandwidth is not sufficient for high-rate data transmission in wireless communication systems. Recently, various bandwidth enhancement techniques have been developed for DRAs, such as

hybrid DRA [10], shaped DRA [11] or stacked DRA [12, 13]. EBG antenna made from metamaterial superstrate is characterized by a high gain and low impedance bandwidth. By exciting EBG antenna with a single DRA source, it is impossible to obtain both a high gain and high bandwidth. Our objective is to enhance the bandwidth and keep a high gain. To achieve these objectives, a new hybrid approach is introduced which uses the concept of metamaterial superstrate for enhancing the gain. Furthermore, a wider bandwidth can be achieved by exciting the EBG structure with multilayer cylindrical dielectric resonator antenna (MCDRA). With the use of this combination, a wide impedance bandwidth ($S_{11} \leq -10\,\text{dB}$) of about 10.5% of the design frequency in between 58.1 and 64.2 GHz is achieved with a gain as high as 18 dBi, which will be largely sufficient to satisfy all the requirements for the 60 GHz wireless communications. This article is organized as follow: in the first part, the antenna design is introduced and two main points are described: the characterization of appropriate excitation source, and the development of the upper surface with the necessary characteristics to achieve the desired gain in a given bandwidth. Experimental validation of the proposed concepts is given in Section 3. Finally, Section 4 presents the conclusion.

2. ANTENNA DESIGN AND SIMULATION RESULTS

A self-explaining flow chart describing the step-by-step design procedure is presented in Figure 1.

The configuration of the proposed antenna is shown in Figure 2, the EBG superstrate, backed by the ground plane, is considered as a Fabry-Perot resonator [14], which is excited by a multilayer cylindrical dielectric resonator antenna (MCDRA).

MCDRA constructed on two dielectric discs with dielectric constant of $(\varepsilon_{r1}) = 6.15$ and $(\varepsilon_{r2}) = 2.2$ from the bottom to top with the same diameter (D) of 3.5 mm, the thicknesses of the discs are $(h_1) = (h_2) = 0.254$ mm. An intermediate substrate is inserted between the ground plane and the MCDRA, it has a thickness $h_3 = 0.127$ mm and a permittivity $\varepsilon_s = 2.2$. This arrangement of MCDRA is placed at the center of a narrow rectangular shaped aperture in the ground plane side of the microstrip line. The slot has a length $L_s = 1.27$ mm and width $W_s = 0.2$ mm and is used to
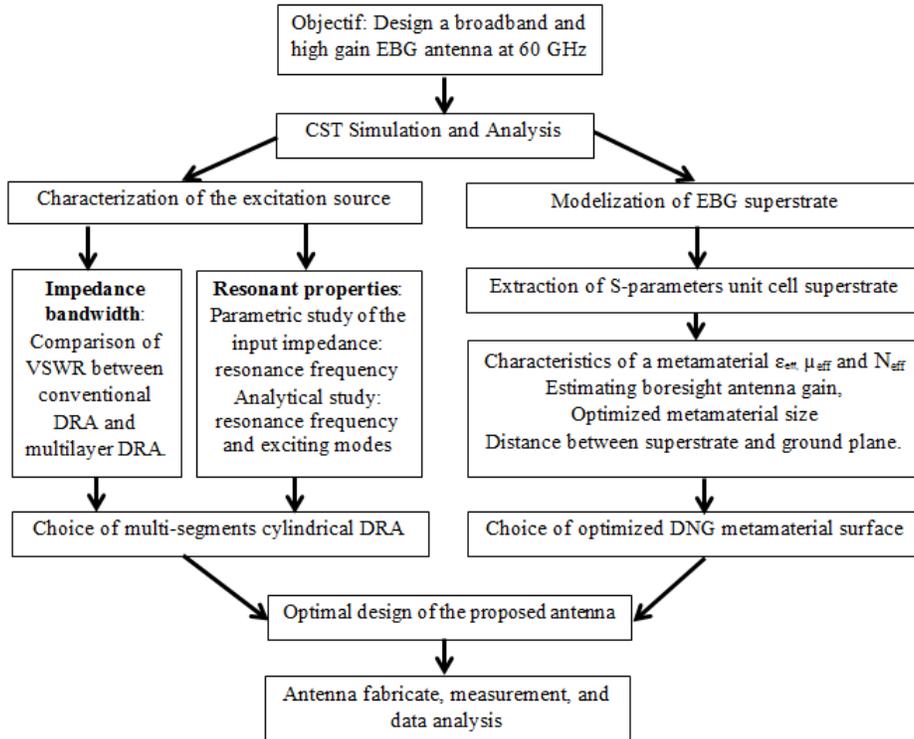

Figure 1. A flow chart explaining the design steps of the proposed antenna.
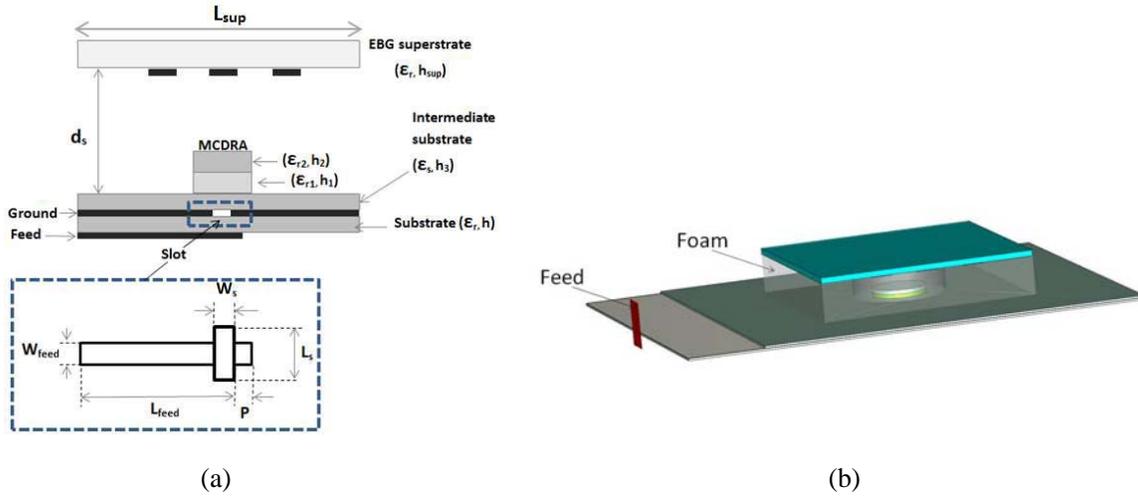
Figure 2. Antenna configuration: (a) side view, dimensions of slot, (b) 3D view of proposed antenna.

Table 1. Geometry parameters of the proposed antenna.

EBG superstrate	$L_{sup} = 14\,\text{mm}$, $W_{sup} = 14\,\text{mm}$ $h_{sup} = 0.381\,\text{mm}$, $d_s = 2.5\,\text{mm}$
Intermediate substrate	$L = 25\,\text{mm}$, $W = 25\,\text{mm}$ $h_3 = 0.127\,\text{mm}$
Dielectric resonators	$D = 3.5\,\text{mm}$ (diameter) $h_1 = 0.254\,\text{mm}$, $h_2 = 0.254\,\text{mm}$
Slot	$L_s = 1.27\,\text{mm}$ $W_s = 0.2\,\text{mm}$
Substrate	$L = 25\,\text{mm}$, $W = 25\,\text{mm}$ $h = 0.127\,\text{mm}$
Fed microstrip line	$L_{feed} = 12.5\,\text{mm}$ $W_{feed} = 0.4\,\text{mm}$

excite the MCDRA. The dielectric substrate of the microstrip line has a dielectric constant of $\varepsilon_r = 2.2$ and thickness $h = 0.127\,\text{mm}$. A $50\,\Omega$ center fed microstrip line having a width $W_{feed} = 0.4\,\text{mm}$ and length $L_{feed} = 12.5\,\text{mm}$ is used to excite MCDRA resonator through the narrow rectangular slot. A tuning stub with length $P = 0.2\,\text{mm}$ is added to the end of the microstrip line to optimize the matching of the antenna. Square EBG superstrate of width $L_{sup} = 14\,\text{mm}$ and permittivity $\varepsilon_r = 10.2$ is placed at a distance $d_s = 2.5\,\text{mm}$ ($d_s = \lambda/2$, as it will be justified in paragraph 2.2 of section 2) of the intermediate substrate and it also has a thickness $h_{sup} = 0.381\,\text{mm}$. A Rohacell foam layer of permittivity 1.07 is sandwiched between base antenna and EBG superstrate to act as a support. The feed line and the ground are modeled as a lossy copper sheets of thickness $t = 0.017\,\text{mm}$. The parameters of the proposed antenna are summarized in Table 1.

EBG is using them as superstrate layers to enhance the gain of small radiation sources such as dielectric resonator antenna. This design procedure has been elaborated following analytical, numerical and experimental trials. Generally, the design of an EBG antenna can be summarized in two main points: the characterization of appropriate excitation source with the same polarization as the desired final antenna, and the development of the upper surface with the necessary characteristics to achieve the desired gain in a given bandwidth.

2.1. Characterization of MCDRA Excitation Source

A very important element in the design of EBG antennas is the excitation source; the choice of this source is based on a set of criteria. Firstly, the polarization of the source must be consistent with that of the bias operation of the entire antenna, and then the resonant frequency of the excitation source must be close to the operating frequency of the EBG antenna.

Our choice to exciting the EBG antenna is focused on multi-segments cylindrical DRA which are recognized for broadband applications. In fact, it is possible to stack multiple resonators so that each

of them can resonate at slightly different frequency resulting in a wider bandwidth.

In this section, the bandwidth and resonant properties of the proposed antenna are investigated. The predicted and optimized performance has been initially done using the simulation and parameterization process available with Computer Simulation Technology (CST) Microwave Studio software.

2.1.1. Bandwidth Comparison

The objective of this experimentation is to determine the increase in the impedance bandwidth, by the use of multilayer cylindrical DRA compared with the conventional cylindrical DRA.

Figure 3(a) shows the geometry of conventional cylindrical DRA with a dielectric constant of $(\varepsilon_{r1}) = 6.15$ and a thicknesses $H = 0.508$ mm. The multilayer cylindrical DRA consist of multiple segments and for this work, a two layers is considered Figure 3(b), where the bottom layer has the same dielectric constant of $(\varepsilon_{r1}) = 6.15$ as that of the conventional DRA and the top layer has a low dielectric constant $(\varepsilon_{r2}) = 2.2$. Thicknesses of the discs are $(h_1) = (h_2) = 0.254$. The simulated voltage standing wave ratios (VSWR) of the conventional cylindrical DRA is compared with that of the multilayer cylindrical DRA in Figure 3(c). The matching frequency range of the conventional cylindrical DRA is found to be from 58.1 to 63 GHz ($VSWR \leq 2$), corresponding to a bandwidth of 8.1%. The matching frequency range of the MCDRA is from 58.1 to 64.2 GHz ($VSWR \leq 2$) corresponding to a bandwidth of 10.5%. The impedance bandwidth is therefore increased by 2.4%. It is expected that the bandwidth of the multilayer cylindrical DRA antenna will be higher than that of the conventional cylindrical DRA antenna.

2.1.2. Resonant Properties

The simulated reflection coefficient (S_{11}) of the EBG antenna is shown in Figure 4.
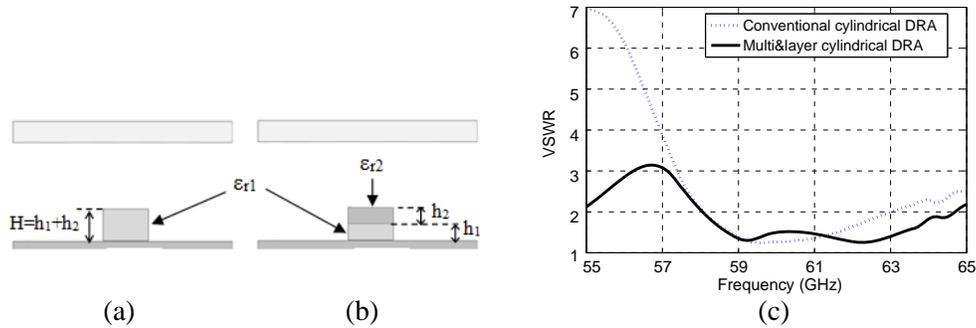

(a)　　　　　　　　(b)　　　　　　　　(c)

Figure 3. (a) Geometry of conventional cylindrical DRA. (b) Geometry of multilayer cylindrical DRA. (c) Comparison of simulated voltage standing wave ratios (VSWR) of the conventional cylindrical DRA and a multilayer cylindrical DRA.
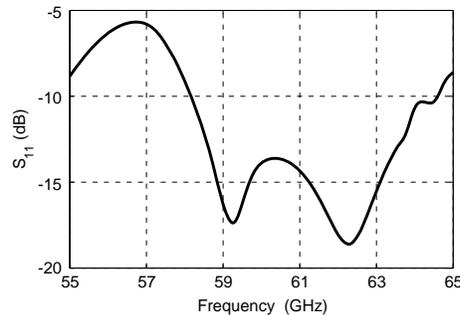

Figure 4. Simulated reflection coefficient of the proposed antenna.

As it can be seen, this antenna shows a dual-resonance broadband match. Two resonances are clearly discernible at 59.1 and 62.1 GHz and the first resonance frequency (near 59 GHz) occurs because of the resonant slot and the second one (near 62 GHz) is due to the MCDRA. To confirm this hypothesis, a short parametric study of the input impedance has been calculated as a function of frequency for different values of slot length, and a radius of MCDRA. Resonance is defined as the frequency at which the real part (resistance) of the input impedance is at maximum and the imaginary part (reactance) goes to zero.

In the first time a parametric study of the proposed antenna without the use of MCDRA is done (proposed antenna excited just by the slot). By taking the combination "resistance peak/reactance zero" as a reference, it can be deduced from Figures 5(a), 5(b), that the first resonance frequency near 59 GHz is due to the slot, since a shift in frequency of the "resistance peak/reactance zero" is noticed when the slot is shortened. After this the proposed antenna is excited by the MCDRA, in Figures 6(a), 6(b), a new resonance appears near 62 GHz and it is interpreted as being caused by the MCDRA since the value of the resistance peak, (near 62 GHz) is clearly affected when the radius of the DRA is changed. This variation is also observed in frequency shift near the "resistance peak/reactance zero", confirming that the DRA is responsible for the second resonance.

The resonant frequency of the slot is also shifted. This is due to coupling effects between the slot and the MCDRA. It is difficult to completely isolate the effects of one in comparison with the other. To confirm the simulation results obtained above for the resonant frequencies and to extract witch modes can be excited within the MCDRA, an analytical study has been conducted to should provide basic information such as resonance frequency and exciting modes [15, 16]. The MCDRA is approximate as a homogenous DRA where the effective permittivity ε_{eff} is calculated using:

$$\varepsilon_{eff} = \frac{H_{eff}}{\dfrac{h_1}{\varepsilon_{r1}} + \dfrac{h_2}{\varepsilon_{r2}} + \dfrac{h_3}{\varepsilon_s}} \tag{1}$$
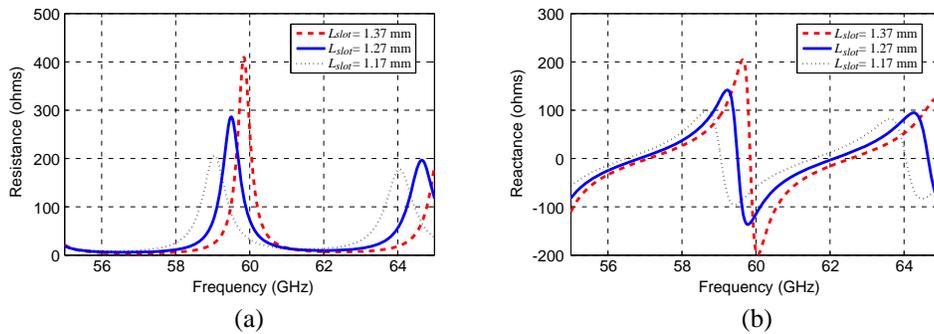

Figure 5. Parametric study of the proposed antenna without the use of MCDRA and changing a length of the slot: (a) resistance R_{in}, (b) reactance X_{in}.
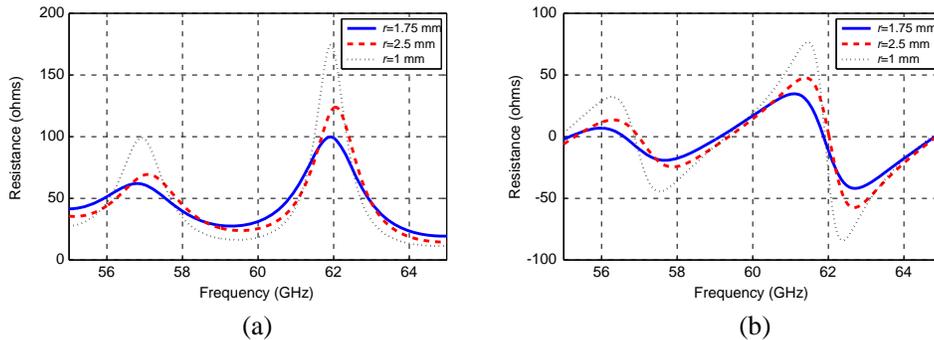

Figure 6. Parametric study of the proposed antenna changing a radius of the MCDRA: (a) resistance R_{in}, (b) reactance X_{in}.

Table 2. Summary of analytical results.

Mode	Resonant frequency (GHz)
$TE_{01\delta}$	48.11
$HE_{11\delta}$	61.99
$EH_{11\delta}$	77.05
$TM_{01\delta}$	70.47

where H_{eff} is the effective height: $H_{eff} = h_1 + h_2 + h_3$. The dimensions of the homogenous DRA are: radius $a = 1.75$ mm, effective height $H_{eff} = 0.635$ mm and effective permittivity $\varepsilon_{eff} = 2.96$. A summary of the results obtained from this study are shown in Table 2. The dominant mode $HE_{11\delta}$ [17, 18] is strongly excited near 62 GHz and the MCDRA is responsible for exciting this mode. A comparison between simulation and analytical calculation for resonant frequency shows a good agreement. It is clear that MCDRA simulated resonance frequency agrees with the value obtained analytically at 62 GHz.

After determining the characterization of the MCDRA excitation source and having determined the dimensions of the antenna, it is time to design the upper interface.
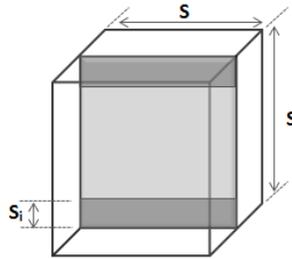
2.2. Modelization of Metamaterial Superstrate

With a suitable design of the superstrate layers placed at an adequate distance from a perfect electric ground plane, it is possible to improve the performance of EBG antennas to obtain a high gain antenna. This superstrate layer must be commercially available, easy to fabricate and compact. For this purpose, metamaterial having simultaneously a negative permittivity and permeability [19, 20] are good candidates. These structures are obtained by the combination of metallic layers and dielectric, one of the best known structures of that type being the FSS superstrate. Various types of FSS elements are used in this configuration such as strip and cross strip patches. In this study, a special superstrate structure composed of thin metallic rods, parallel to the E field has been used. The unit cell geometry of the proposed thin planar metamaterial is shown in Figure 7. Two parallels metallic strip has been printed on a $Duroid^{©}$ board having 0.381 mm thickness, relative permittivity of 10.2, and a loss tangent $\tan\delta = 0.003$. The size of the elements has been chosen in a way to provide a sufficiently high reflectance for frequencies near 60 GHz. ($S_i = 0.54$ mm, $S = 2.5$ mm). The CST microwave studio was used to obtain the reflection and transmission coefficients for a normal incident plane wave to the cell plane.

The magnitudes and phases of the S-parameters (S_{11} and S_{21}) are shown in Figures 8(a), 8(b), respectively.

One of the most important parameters for the adjustment of the resonance frequency is the distance between the superstrate layer and ground plane; this distance can be deduced from the resonance condition given by [21]:

$$d_s = \frac{c}{2f} \left(\frac{\Phi_{EBG} + \Phi_{GND}}{2\pi} \right) \tag{2}$$

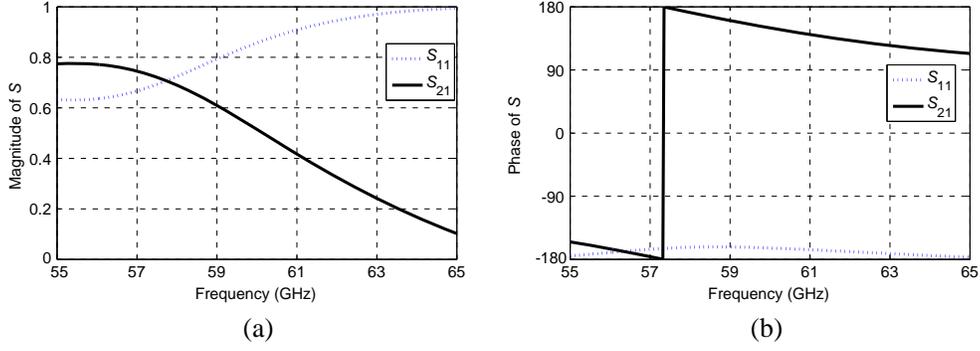**Figure 7.** Dimension of the metamaterial superstrate unit cell.

Figure 8. Simulated reflection (S_{11}) and transmission (S_{21}) responses of the metamaterial superstrate unit cell shown in Figure 7: (a) magnitude, and (b) phase.

where c and f are respectively the velocity of light and the operating frequency, in the Fabry Perot Cavity antenna system Φ_{EBG} is the reflection phase of the metamaterial superstrate and Φ_{GND} is the reflection phase of the ground plane. At 60 GHz, the value Φ_{EBG} is 170° (Figure 8(b)), the ground plane is a perfect electric conductor; therefore, Φ_{GND} is equal to 180°. The value of d_s is found to be 2.4 mm because manufacturing constraints is chosen to be 2.5 mm. Once the study of the metamaterial superstrate reflectivity has been done, the second step consists in extracting effective parameters. There are various approaches to calculate the effective parameters of the substrate such as permittivity, permeability, refractive index and the effective impedance. The most popular one is by extraction from transmission and reflection characteristics of a metamaterial based on the (Kramers-Kronig) algorithm [22]. The effective impedance (Z_{eff}) and effective refractive index (N_{eff}) are retrieved from the S-parameters, and then effective permittivity(ε_{eff}) and permeability (μ_{eff}) are computed from (N_{eff}) and (Z_{eff}) values.

The coefficients (S_{11}) and (S_{21}) are related to the refractive index (N_{eff}) and the impedance (Z_{eff}) of the material, by the following relations:

$$Z_{eff} = \pm\sqrt{\frac{(1 + S_{11}) - S_{21}^2}{(1 - S_{11}) - S_{21}^2}} \tag{3}$$

$$N_{eff} = \frac{1}{k_0 d} \{\text{Im}\left[\ln(T)\right] + 2m\pi - i\text{Re}\left[\ln(T)\right]\} \tag{4}$$

$$T = \frac{S_{21}}{1 - S_{11}R} \tag{5}$$

$$R = \frac{Z_{eff} - 1}{Z_{eff} + 1} \tag{6}$$

where R is the complex wave impedance, m can be any integer, k_0 is the free-space wavenumber, and d is thickness of unit cell. The generic form of the effective permittivity can be expressed with the following:

$$\varepsilon_{eff} = \frac{N_{eff}}{Z_{eff}} \tag{7}$$

To get the double negative (DNG) behavior, the magnetic resonance offering the negative permeability should also be achieved. The expression for the effective permeability is given by the following:

$$\mu_{eff} = N_{eff} Z_{eff} \tag{8}$$

As shown in Figures 9(a), 9(b) real parts of permittivity and permeability are simultaneously negative in the range of 57.5 GHz to 61.5 GHz. The real part of the effective refractive index, Figure 9(c), shows a plateau at the frequency 57.5 GHz, exhibits a negative value on the frequency band (57.5–61.5 GHz), and it takes an almost constant value around (-4), the region where the index is negative corresponds to the frequency band where both ε_{eff} and μ_{eff} are simultaneously negative. It can therefore be said that the gain is maximum in this frequency band Figure 9(d).
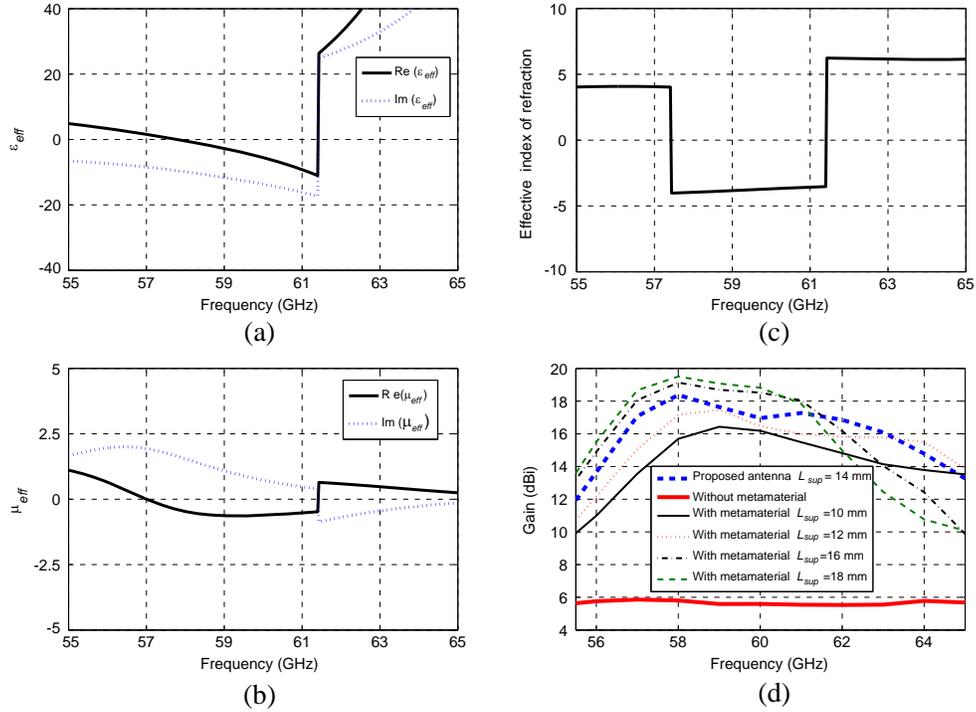
Figure 9. Extracted effective parameters of the metamaterial superstrate unit cell based on Kramers Kronig relations. (a) Relative permittivity (solid line: real part, dashed line: imaginary part). (b) Relative permeability (solid line: real part, dashed line: imaginary part). (c) Real part of the effective refractive index (N_{eff}) as a function of frequency for $m = 0$. (d) Comparative curves of gain versus frequency for different metamaterials size.

The expression for estimating boresight antenna gain, relative to that of the primary antenna, has been defined as [21]:

$$G = \frac{1 + \Gamma}{1 - \Gamma} \tag{9}$$

where Γ is the reflection coefficient of the metamaterial superstrate unit cell. In this case the primary source MCDRA has a gain of 5.5 dBi, when an infinite 2D metamaterial superstrate is placed above the ground plane (metamaterial is treated as an infinite periodic structure, thus reducing the problem size to a single unit cell); the reflection coefficient is thus 0.84 at 60 GHz. The estimated additional gain is about 11.5 dBi and a total antenna gain increase as high as 17 dBi has been obtained. However, the infinite metamaterial structure is a theoretical case since, in practice, all periodic structures have finite size. To find the minimal number of unit cell which is necessary to approach the infinite case, a parametric study of the gain versus frequency for different size of metamaterials has been conducted. From Figure 9(d), it is noticed that the gain is considerably increased (by 3 dBi from 16.5 to 19.5 dBi) when the size of metamaterials change from 12 mm to 18 mm and the maximum gain is achieved for a superstrate size of 18 mm, achieving 19.5 dBi over a frequency range of 56.3 to 61.5 GHz (3 dBi lower than the maximum value). Examination of the curves in the various frequency bands show that the gain achieved with a metamaterial size of 14 mm ($\sim 3\lambda$) consisting of a 5×6 array (30 unit cells), has an excellent agreement with gain obtained from the infinite metamaterial structure (17 dBi at 60 GHz).

The aim is to design an antenna with the smallest metamaterials superstrate that can achieve an appreciable gain, as stable as possible across the unlicensed ISM frequency band at 60 GHz (57–65 GHz). To meet these objectives the size of the metamaterial is chosen to be 14 mm, in order to obtain the optimum design. The simulated gain of the MCDRA with the metamaterial size of 14 mm was enhanced by about 13 dBi over the antenna without a metamaterial layer; the maximum gain being boosted to 18 dBi.

After determining the permittivity, permeability, and the size of the upper superstrate and selecting an adequate source of excitation, the performance of the proposed antenna can now be established. The integral design of the proposed antenna having a directional radiation pattern is shown in Figure 10.

3. EXPERIMENTAL RESULTS

In order to validate the simulation results, the antenna prototype of Figure 2, has been fabricated and measured. A photographs of the fabricated antenna are shown in Figure 11. First, the measured reflection coefficient is plotted versus frequency in Figure 12(a). For comparison and verification purposes, numerical simulations done with CST microwave studio, which is based on the finite integration method, are also plotted. As it can be seen the matching frequency range of the fabricated antenna is from 59 GHz to 67 GHz, corresponding to a bandwidth of 13.3%, large, enough to cover the ISM band. Two resonances are clearly discernible and, as it was explained, the first resonance near the 60.5 GHz is due to the resonant coupling slot, a second negative peak near 64 GHz it is the result of the excitation of the hybrid mode of MCDRA.

It is noted that there is a frequency shift of about 1.3 GHz, between the simulated and measured results. This shifting is due to the combined effect of connector losses and the insertion of a foam layer of permittivity 1.07 between intermediate substrate and metamaterial superstrate. The simulated and measured radiation gains of the proposed antenna as a function of frequency is illustrated in Figure 12(b).
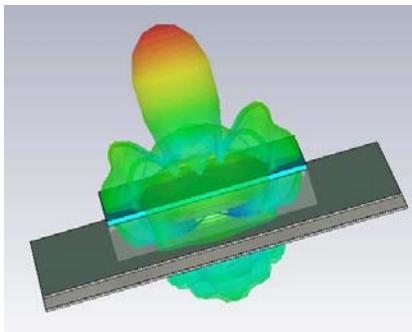

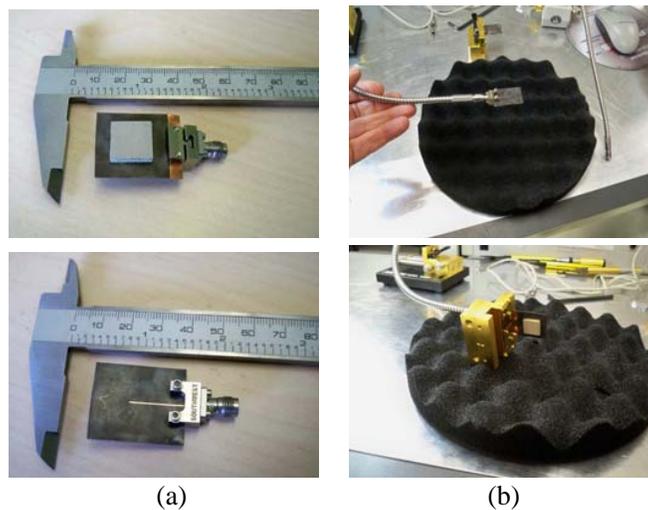**Figure 10.** 3D proposed antenna design and 3D radiation pattern visualization.

(a) (b)

Figure 11. (a) Photographs of the fabricated prototype. (b) Set-up for the measurements of the S_{11} parameter.
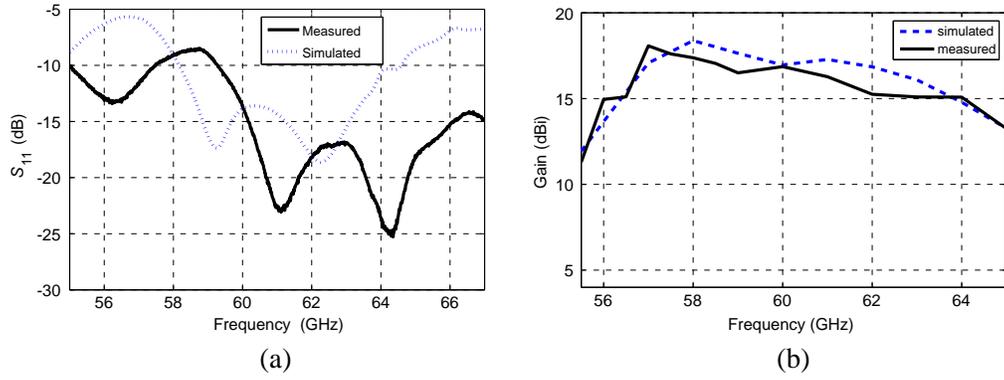
Figure 12. (a) Measured and simulated reflection coefficient of proposed antenna S_{11}. (b) Measured and simulated gain of proposed antenna.
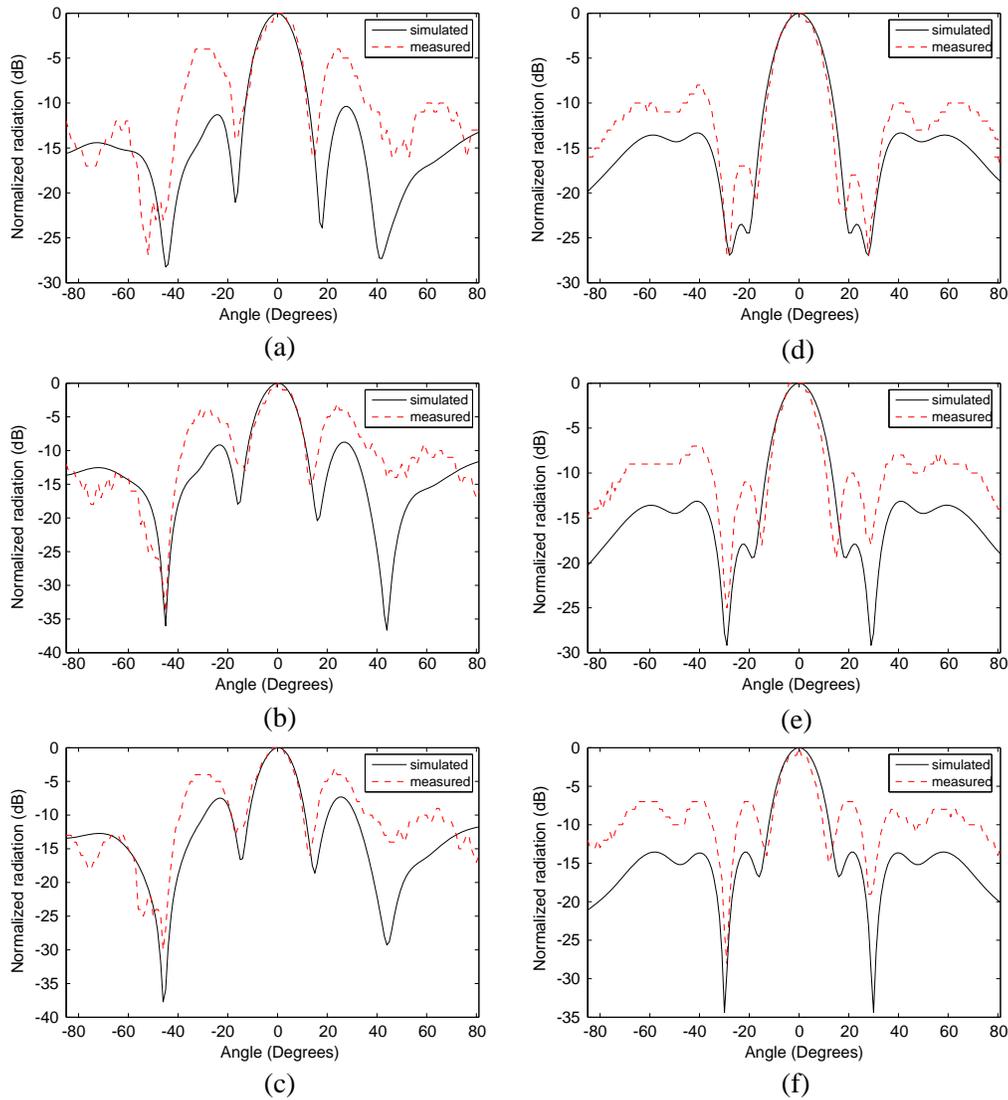

Figure 13. Measured and simulated radiation patterns of the prototype: H plane at ((a) 59 GHz, (b) 60 GHz, and (c) 61 GHz). and E plane at ((d) 59 GHz, (e) 60 GHz, and (f) 61 GHz).

Table 3. Performance comparison between the proposed antenna and some existing antennas.

Ref	Bandwidth	Gain	Dimensions mm^3	Process	Type
[23]	10 % (57–63) GHz	17 dBi	20 × 20 × 6.88	Prototype	4 layers grid superstrate suspended over a patch antenna
[24]	6.8 % (57–61.1) GHz	16 dBi	30 × 30 × 3.46	Prototype	Aperture coupled patch antenna with superstrate
[24]	17.6 % (56.4–67.3) GHz	14.44 dBi	10 × 10 × 3.5	Design	Rectangular dielectric resonator covered with superstrate
[26]	0.66% (59.8–60.2) GHz	20.4 dBi	24 × 24 × 3.5	Design	A dipole located in ground plane covered by a metallic FSS
Proposed in this paper	10.5% (58.1–64.2) GHz	18 dBi	25 × 25 × 3.14	Prototype	A multilayer cylindrical DRA covered with metamaterial superstrate

The most appealing feature of this antenna resides in its high gain, gain around 18 dBi, with a difference of 3 dBi between the lowest and the highest value. The minimum gain is about 15 dBi at 64 GHz while the maximum gain is 18 dBi at 59 GHz respectively. It can be noted that the gain is almost stable over the frequency range of 59 GHz to 64 GHz. It is obvious that simulation and measured results confirm that the obtained have a high gain meets the design goal.

The measured and simulated E and H plane radiation patterns at 59 GHz, 60 GHz and 61 GHz are shown in Figures 13(a)–13(f). These result shows that the main lobe of the proposed antenna is highly directive and the maximum gain achieved at this frequency is about 18 dBi. It can be noted that the simulated radiation patterns are found to be stable and in good agreement with measured ones. The results correspond to the objective to obtained a highly directional antenna.

4. CONCLUSION

As a summary, a comparison Table 3 is presented which shows the itemized performance characteristics in terms of a size, bandwidth and maximum gain, between the proposed antenna and some other existing antennas using metamaterial superstrate. It is clear from the table that the proposed antenna has not only smaller size, but also exhibits better impedance bandwidth and high gain which can be easily fabricated. This paper has shown how a broadband highly directive, multilayer cylindrical dielectric resonator antenna covered with double negative metamaterial superstrate, for millimeter-wave operation can be successfully developed. The prototype was fabricated using printed circuit technology, and the results show a good agreement between measurements and simulations. More than 10.5% bandwidth was achieved (from 58.1 to 64.2 GHz) and a gain 18 dBi, which is almost constant in the operating band. This is an enhancement of 12 dBi compared to a classical DRA without superstrate, with the obtained results; the proposed antenna is attractive and can be practical for underground communications systems.

REFERENCES

1. Rappaport, T. S., J. Murdock, and F. Gutierre, "State of the art in 60-GHz integrated circuits and systems for wireless communications," *Proceedings of the IEEE*, Vol. 99, No. 8, 1390–1436, 2011.

2. Smulders, P. F. M., "60 GHz radio: Prospects and future directions," *Proceedings of the IEEE Symposium Benelux Chapter on Communications and Vehicular Technology*, 1–8, Eindhoven, Netherlands, 2003.

3. Petosa, A., A. Ittipiboon, Y. M. Antar, and D. Roscoe, "Recent advances in dielectric resonator antenna technology," *IEEE Antennas and Propagation Magazine*, Vol. 40, No. 3, 35–48, Jun. 1998.

4. Vettikalladi, H., O. Lafond, and M. Himdi, "High-efficient and high-gain superstrate antenna for 60-GHz indoor communication," *IEEE Antennas Wireless Propagat. Lett.*, Vol. 8, 1422–1425, 2009.

5. Thvenot, C. and R. Jecko, "Directive photonic band gap antenna," *IEEE Trans. on Microwaves Theory and Tech.*, Vol. 47, 2115–2122, Nov. 1999.

6. Denidni, T. A., Y. Coulibaly, and H. Boutayeb, "Hybrid dielectric resonator with circular musroom like stucture for gain improvement," *IEEE Trans. Antennas Propag.*, Vol. 57, No. 4, 1043–1049, Apr. 2009.

7. Elkarkraoui, T., G. Y. Delisle, N. Hakem, and Y. Coulibaly, "New hybrid design for a broadband high gain 60-GHz dielectric resonator antenna," *7th European Conference on Antennas and Propagation (EUCAP'2013)*, 2379–2382, Gothenburg, Sude, 2013.

8. Chen, X., T. M. Grzegorczyk, B.-I. Wu, J. Pacheco, and J. A. Kong, "Robust method to retrieve the constitutive effective parameters of metamaterials," *Phys. Rev.*, Vol. 70, No. 1, 016608.17, 2004.

9. Saenz, E., R. Gonzalo, I. Ederra, J. C. Vardaxoglou, and P. de Maagt, "Resonant meta-surface superstrate for single and multi-frequency dipole antenna arrays," *IEEE Trans. Antennas Propag.*, Vol. 56, 951–960, 2008.

10. Esselle, K. P. and T. S. Bird, "A hybrid-resonator antenna: Experimental results," *IEEE Trans. Antennas Propag.*, Vol. 53, 870–871, 2005.

11. Kishk, A., Y. Yin, and A. W. Glisson, "Conical dielectric resonator antennas for wide-band applications," *IEEE Trans. Antennas Propag.*, Vol. 50, 469–474, 2002.

12. Ge, Y., K. P. Esselle, and T. S. Bird, "A wide band probe-fed stacked dielectric resonator antenna," *Microwave and Optical Technology Letters*, Vol. 48, No. 8, 1630–1633, Aug. 8, 2006.

13. Huang, W. and A. A. Kishk, "Compact wideband multi-layer cylindrical dielectric resonator antennas," *IET Microw. Antennas Propagation*, Vol. 1, 998–1005, Oct. 2007.

14. Kaklamani, D. I., "Full-wave analysis of a Fabry-Parot type resonator," *Progress In Electromagnetics Research*, Vol. 24, 279–310, 1999.

15. Walters, K. A. and G. W. Hanson, "Resonant frequency calculation for inhomogeneous dielectric resonators using volume integral equations and face-centered node points," *Microwave and Optical Technology Letters*, Vol. 32, No. 5, 356–359, 2002.

16. Mongia, R. K. and P. Bhartia, "Dielectric resonator antennas a review and general design relations for resonant frequency and bandwidth," *International Journal of Microwave and Millimeter-wave Computer-aided Engineering*, Vol. 4, No. 3, 230–247, Mar. 1994.

17. Long, A., M. W. McAllister, and L. C. Shen, "The resonant cylindrical dielectric resonator antenna," *IEEE Trans. Antennas Propag.*, Vol. 31, No. 3, 406–412, May 1983.

18. Glisson, A. W., D. Kajfez, and J. James, "Evaluation of modes in dielectric resonators using a surface integral equation formulation," *IEEE Trans. on Microwaves Theory and Tech.*, Vol. 31, No. 12, 1023–1029, 1983.

19. Han, T. C., M. K. A. Rahim, T. Masri, and M. N. A. Karim, "Left handed metamaterial design for microstrip antenna application," *Microwave Conference, Asia-Pacific Microwave Conference*, 1–4, Bangkok, Thailand, 2007.

20. Ziolkowski, R. W., "Design, fabrication, and testing of double negative metamaterials," *IEEE Trans. Antennas Propag.*, Vol. 51, 1516–1529, 2003.

21. Feresidis, A. P. and J. C. Vardaxoglou, "High gain planar antenna using optimized partially reflective surfaces," *IEE Proceedings — Microwaves, Antennas and Propagation*, Vol. 148, No. 6, 345–350, Dec. 2001.

22. Szabo, S., G.-H. Park, R. Hedge, and E.-P. Li, "A unique extraction of metamaterial parameters based on Kramers-Kronig relationship," *IEEE Trans. on Microwaves Theory and Tech.*, Vol. 58, No. 10, 2646–2653, Oct. 2010.

23. Franson, S. J. and R. W. Ziolkowski, "Giga-bit per second data transfer in high-gain metamaterial structures at 60 GHz," *IEEE Trans. Antennas Propag.*, Vol. 57, No. 10, 2913–2925, 2009.

24. Vettikalladi, H., L. Le Coq, O. Lafond, and M. Himdi, "High-effcient slot-coupled superstrate antenna for 60 GHz WLAN applications," *Proceedings of the Fourth European Conference on Antennas and Propagation (EuCAP)*, 1–5, 2010.

25. Coulibaly, Y., M. Nedil, I. Ben Mabrouk, L. Talbi, T. A. Denidni, "High gain rectangular dielectric resonator for broadband millimeter-waves underground communications," *Publication on Canadian Conference Electrical and Computer Engineering (CCECE)*, 1088–1091, 2011.

26. Hosseini, S. A., F. Capolino, and F. De Flaviis, "Design of a single-feed 60 GHz planar metallic Fabry-Perot cavity antenna with 20 dB gain," *Proceedings of the IEEE International Workshop on Antenna Technology (iWAT' 09)*, 1–4, Santa Monica, Calif, USA, Mar. 2009.